www.ptcer.pl/mccm

MATERIAŁY CERAMICZNE /CERAMIC MATERIALS/, 64, 2, (2012), 168-171

Mechanical properties and microstructure of 1Y2Nd-TZP/20 vol.% alumina nanocomposites

Frank Kern

University of Stuttgart, Institute for manufacturing technology of ceramic components and composites IFKB, Allmandring 7B, D-70569 Stuttgart, Germany
e-mail: frank.kern@ifkb.uni-stuttgart.de

Abstract

Zirconia based composites are frequently used in mechanical and biomedical components demanding high strength and toughness. In the present study, alumina toughened zirconia ceramics were manufactured from 1 mol.% yttria 2 mol.% neodymia stabilized TZP blended with 20 vol.% alumina by hot pressing at 1250-1450°C/1 h/60 MPa. Mechanical properties, phase composition and microstructure were investigated. The co-stabilized ATZ material exhibits a combination of high 4-pt bending strength of 1300 MPa and very high fracture resistance of 11 MPa·√m. The threshold stress intensity of 5 MPa·√m indicates a high resistance to subcritical crack growth. The microstructure shows a homogeneous dispersion of alumina grains in a bimodal zirconia matrix consisting of transformable fine grains and untransformable large cubic grains. Most favourable properties are developed at sintering temperatures of 1350–1400°C, at higher temperature the material decomposes to monoclinic and cubic losing its high strength and toughness.

Keywords: Structural ceramics, Phase transformation, Deformation and fracture, Microstructure - final

WŁAŚCIWOŚCI MECHANICZNE I MIKROSTRUKTURA NANOKOMPOZYTÓW 1Y2Nd-TZP/20% OBJ. KORUND

Kompozyty bazujące na dwutlenku cyrkonu stosowane są często do wykonywania elementów mechanicznych i biomedycznych wymagających wysokiej wytrzymałości i odporności na pękanie. W ramach prezentowanej pracy wytworzono ceramikę cyrkoniową wzmocnioną korundem, wykorzystując TZP stabilizowane dodatkami 1% mol. tlenku itru i 2% mol. tlenku neodymu, które zmieszano z korundem w ilości 20% obj. i konsolidowano drogą prasowania na gorąco w 1250–1450°C przez 1 h pod ciśnieniem 60 MPa. Zbadano właściwości mechaniczne, skład fazowy i mikrostrukturę. Współstabilizowany materiał ATZ pokazał kombinację wysokiej 4-punktowej wytrzymałości wynoszącej 1300 MPa i bardzo wysokiej odporności na pękanie - 11 MPa·√m. Progowa intensywność naprężeń wynosząca 5 MPa·√m wskazuje na wysoką odporność na podkrytyczny wzrost pęknięć. Mikrostruktura pokazuje jednorodne rozproszenie ziaren korundu w dwumodalnej osnowie cyrkoniowej składającej się z przemienialnych drobnych ziaren i nieprzemienialnych, dużych, ziaren o strukturze regularnej. Najlepsze właściwości uzyskuje się w temperaturach spiekania z przedziału 1350-1400°C; przy wyższych temperaturach materiał rozkłada się na fazy jednoskośną i regularną tracąc swoją wysoką wytrzymałość i odporność na pękanie.

Słowa kluczowe: ceramika konstrukcyjna, przemiana fazowa, deformacja i pękanie, mikrostruktura finalna

1. Introduction

Alumina toughened zirconia (ATZ) composites were designed to combine the high toughness of TZP (tetragonal zirconia polycrystals) with enhanced hardness and strength for demanding engineering or biomedical applications [1]. The commercially available ATZ materials consisting of 3Y-TZP and 20-30 vol.% alumina do reach outstanding strength of up to 2 GPa but only moderate toughness of 4.5-5 MPa·√m [2]. Shifting from a Y-TZP to a Ce-TZP matrix increases toughness at the expense of strength [3]. Concepts for ATZ materials like hexaaluminate platelet reinforcements [4], replacing of co-precipitated by coated zirconia powder [5] and nanocomposite Ce-TZP/alumina [6] have led to considerable improvements. The recently published work on Ce-TZP/spinel composites presented a strength of 930 MPa coupled with a toughness of >15 MPa·√m [7]. Alternative stabilizer systems for TZP like yttria-neodymia Y-Nd-TZP coupled with powder coating technology have been introduced by Vleugels [8] and applied as a matrix material in composite materials together with e.g. WC [9] or alumina [10]. Recent work has shown that phase separation to a stabilizer rich cubic phase and an extremely transformable tetragonal phase happens in YNd2-TZP at low sintering temperature and causes the high toughness of the material. [11] The aim of this study is to obtain a deeper understanding of the evolution of microstructure, phase composition and mechanical properties of Y-Nd-TZP/alumina composites with variations in sintering conditions.

2. Experimental

The starting powders for this study were unstabilized zirconia VP-Ph (Evonik, Germany, S_{BET} = 60 m²/g) and alumina APA0.5 (Ceralox, USA, S_{BET} = 8 m²/g). The zirconia was coated via the nitrate route with 1 mol.% yttria and 2 mol.% neodymia basically following the procedure of Vleugels [8]. A coating procedure adapted to ultrafine zirconia was previ-

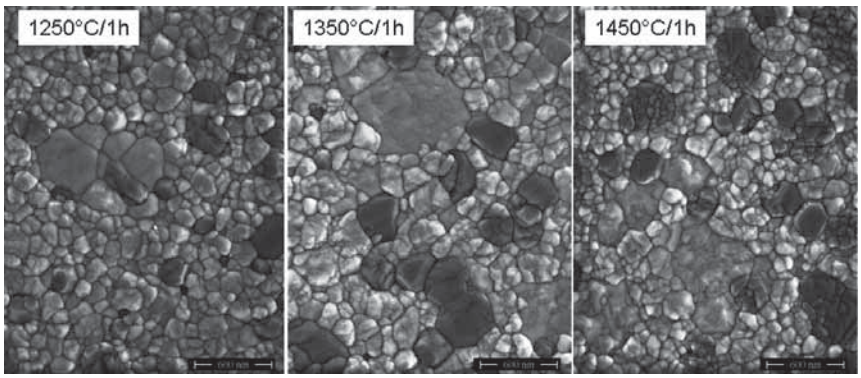

Fig. 1. SEM images of polished and thermally etched surfaces of ATZ sintered at 1250°C (a), 1350°C (b) and 1450°C (c).

ously described in detail by the author [12]. The resulting calcined powder was blended with 20 vol.% alumina and milled for 4 h in 2-propanol using Y-TZP balls (d = 1 mm). The resulting ATZ blend was dried and screened. Samples were consolidated by hot-pressing (KCE, Germany) at 1250°C-1450°C for 1 h under 60 MPa axial pressure. The resulting plates with a dimension of 42 mm x 22 mm x 2 mm were lapped and polished with diamond suspension and cut into bending bars. Sides and edges of the bars were carefully ground and polished to eliminate machining defects. The microstructure of polished and thermally etched surfaces (1200 °C/ 10 min/ air) with a conductive PdPt coating was investigated by SEM (Zeiss, Germany) in SE mode at 3 kV acceleration voltage. The phase composition was measured on polished surfaces and fracture faces by integrating the areas of monoclinic and tetragonal XRD reflexes in the 27-33° 2θ-range applying the calibration curve of Toraya [13] (Bruker D8, Germany, CuKα, graphite monochromator). Mechanical properties measurement included measurement of Vickers hardness HV10 and HV0.1, determination of the indentation modulus E_{IND} and the measurement of 4pt bending strength in a setup with 10 mm inner and 20 mm outer span at a crosshead speed of 2.5 mm/min. Fracture toughness was determined by stable indentation crack growth in flexure in the same 4pt setup at a crosshead speed of 5 mm/min using bending bars indented with 4 HV10 indents. The procedure was proposed by Braun [14] and refined by Dransmann [15]. The experimental procedure followed closely the protocol described by Benzaid [6]. Samples were pre-indented with four HV10 indents each at 2 mm distance in the middle of the tensile side of a bending bar. The samples were then stored for 2 weeks to allow the cracks to grow subcritically to a stable extension. Samples were tested in the same 4pt setup at a crosshead speed of 5 mm/min. They were initially loaded with 30% of their residual strength. The load was subsequently increased in 50-100 MPa increments until fracture. The length of the cracks perpendicular to the sides was measured after each loading step. A plot of the applied stress intensity $K_{appl} = \psi \cdot \sigma \cdot \sqrt{c}$ versus the residual indentation stress intensity $K_{res} = P \cdot c^{-1.5}$ allows the determination of the subcritical stress intensity K_0. If $K_{res} > K_{appl}$ no crack growth occurs. The onset of crack growth visible by the kink in the curve is the value $K_{appl,0}$. The fracture toughness is obtained at the intercept of the straight linear part with the slope χ starting from the kink and the ordinate. The threshold K_0 is given by $K_0 = K_{IC} - K_{appl,0}$. The parameters for the calculation are the indentation load P = 98.1 N, the crack geometry parameter ψ = 1.27, the measured crack length c in μm, and the stress σ in MPa. As Lube and Fett have shown that in case of material with R-curve behaviour the extrapolation to the ordinate intercept can lead to unrealistically high values for the fracture resistance [16]. In a conservative approach the highest measured toughness values of the stable indentation crack growth in bending were chosen as the real fracture resistance.

3. Results

Fig. 1 shows the microstructure of ATZ sintered at 1250, 1350 and 1450°C. The dark alumina grains are well distributed in the zirconia matrix. The zirconia clearly shows a bimodal structure consisting of finer grains with a structured surface and larger grains with a flat surface. Isolated alumina grains do not grow, the grain growth thus mainly affects the zirconia. The size of the smaller zirconia grains increases from 150-300 nm at 1250°C to 200-400 nm at 1350°C. The larger grains seem to grow by coalescence of pre-existing smaller units and do not grow into the fine grained environment. At the highest sintering temperature, there is an apparent refinement of the zirconia and an apparent disintegration of the alumina into smaller units, the latter may occur by reaction of alumina with neodymia forming aluminates as observed by Liu [17]. The formerly flat large zirconia grains show a structured surface. The onset of this behaviour can be detected in ATZ sintered at 1400°C (not shown).

The phase composition of the ATZ is shown in Fig. 2. The monoclinic content in the polished surfaces representing the bulk composition exhibits a minimum of 6 vol.% at 1300°C. Then the monoclinic content rises exponentially with rising sintering temperature. While the monoclinic content at 1400°C is ~20 vol.% and close to the stress-neutral state [5], the final rise indicates the decomposition of the material already detected in SEM images. The transformability is very high and shows two maxima of ~ 50 vol.% at 1250°C and 1350°C. Above a sintering temperature of 1350°C transformability tends to decline. At 1300°C the tetragonal (101) reflex located at 30.3° 2θ tends to develop a shoulder which at sintering temperatures ≥1350°C develops into a separate reflex at 29.9° 2θ (Fig. 3). This reflex shows a rising intensity with rising sintering temperature. The additional reflex is the (111) reflex of a neodymia (and yttria) rich cubic zirconia

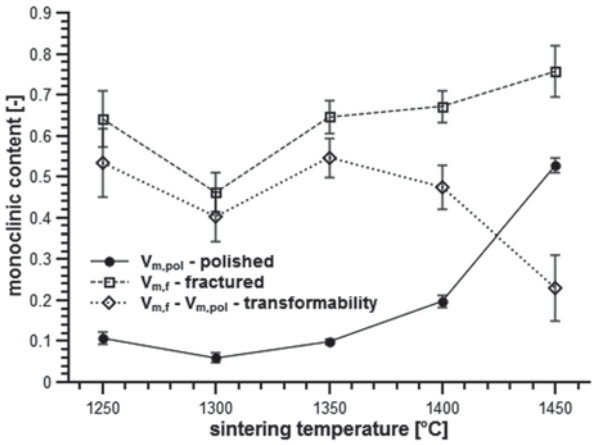

Fig. 2. Monoclinic contents in polished surfaces and fracture faces of ATZ sintered and resulting transformability vs. sintering temperature.

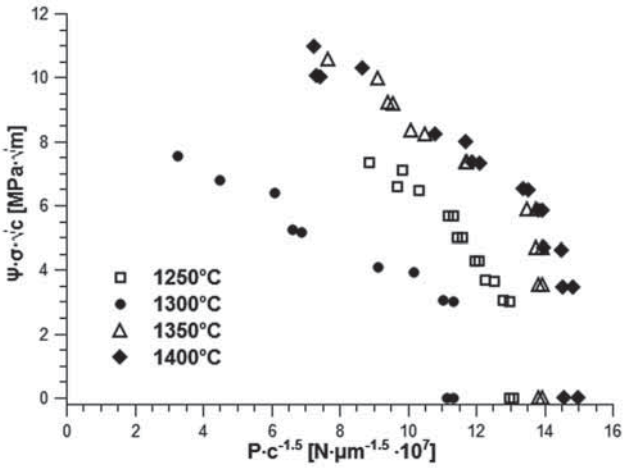

Fig. 4. Bending strength σ_{4pt}, fracture resistance and threshold stress intensity K_0 of ATZ vs. sintering temperature.

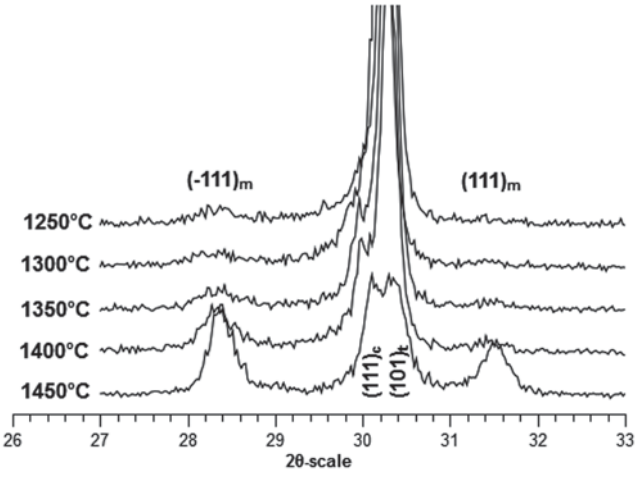

Fig. 3. XRD traces in the 27–33° 2θ-range of polished ATZ surfaces vs. sintering temperature.

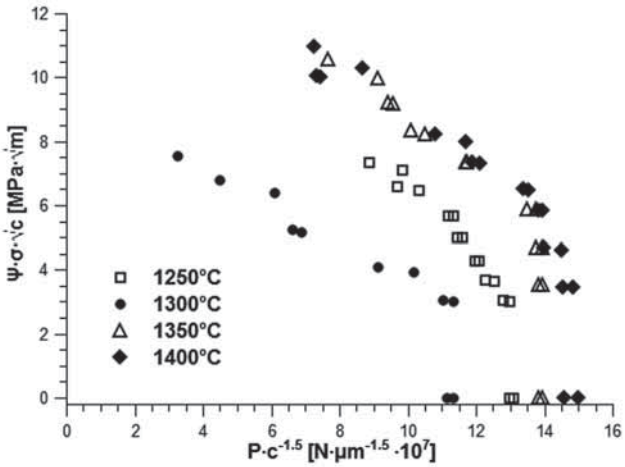

Fig. 5. Linearized plot of stable indentation crack growth in bending experiments performed on ATZ sintered at (1250–1400)°C.

[17]. The fact that the reflex remains in the fracture phase while the $(101)_t$ reflex declines proves that the phase is non transformable. At the highest sintering temperature most of the samples are already predominantly cubic and monoclinic, thus the reduction in transformability is not surprising.

Recent results on YNd2-TZP have shown that the stabilizer contents in the large grains are approximately four times higher than in the fine grain matrix [11]. The occurrence of cubic coincides with the steep rise in toughness, phase separation into a tetragonal phase with low stabilizer content and high transformability and a stabilizer rich phase taking up the excess neodymia (and yttria) seems to be the driving force for toughening. Compared to co-precipitated Y-TZP the phase separation occurs at significantly lower temperature and dwell [18].

The mechanical properties strength, toughness and threshold stress intensity are shown in Fig. 3. Fig. 4 shows the linearized plot of stable indentation crack growth in bending experiments according to Benzaid [6].

The ATZ reaches a peak strength of > 1300 MPa. Fracture resistance values rises from 7 MPa·√m at 1250°C to 11 MPa·√m at 1400°C sintering temperature. At 1450°C a sharp drop observed. Comparing the trends in Figs. 1 and 3 reveals a synchronized devolution of strength, toughness and transformability. The threshold stress intensity K_0 increases linearly from 4 MPa·√m at 1250 °C to 5.3 MPa·√m at 1400°C

Table 1. Density, indentation modulus and microhardness of 1Y-2Nd-TZP/20% alumina composites versus sintering temperature.

Sintering temperature T [°C]	Density [g/cm³]		Indentation modulus [GPa]		Microhardness HV0.1 [-]	
1250	5.604	± 0.032	268	± 3	1630	± 37
1300	5.684	± 0.031	271	± 2	1742	± 28
1350	5.704	± 0.012	271	± 1	1707	± 17
1400	5.711	± 0.017	275	± 2	1663	± 16
1450	5.719	± 0.01	280	± 1	1628	± 15

and markedly exceeds the typical value of ~3 MPa·√m for Y-TZP [15]. In the sample sintered at 1450°C which showed a strong deterioration of the microstructure and phase composition strength and toughness are reduced.

Table 1 contains values of density, indentation modulus and microhardness HV10. The initial increase in density between 1250°C and 1300°C indicates a change in phase composition as the microstructure at this sintering temperature is fully dense.

4. Discussion

An interpretation of the results shown above must start with the changes in phase composition which is the driving force for microstructural changes and the prerequisite for the favourable mechanical properties. Phase diagrams for the binary subsystems Y_2O_3-ZrO_2 [20] and Nd_2O_3-ZrO_2 [21] show that in the selected sintering temperature range location of the tetragonal /tetragonal+cubic t/(t+c) phase boundary is at 2-2.5 mol-% yttria and 1-1.5 mol-% neodymia. The starting composition is thus supersaturated with neodymia. As the t+c field represents a miscibility gap phase separation is thermodynamically favored. The starting powder was made by a coating process, the stabilizer distribution is therefore inhomogeneous from the beginning which should accelerate phase separation. The separation of excess stabilizer in cubic grains depletes the tetragonal grains from stabilizer and increases transformability and fracture toughness. The phase separation is confirmed by SEM and XRD. An ATZ composite with no monoclinic would develop tensile cooling stress in the zirconia matrix due to CTE mismatch of alumina and zirconia. This tensile stress can transform the most transformable fraction during cooling and form monoclinic phase accompanied by volume expansion of ~5–6 %. Tensile stress in the matrix is thus reduced or may even shift to compressive above a stress neutral state at ~ 15% monoclinic [5]. Compressive stress in the matrix will add to the applied stress and thus increase the strength. The compressive stress will also delay transformation of zirconia and thus raise the threshold stress intensity. The surplus of threshold stress intensity of 2 MPa·√m compared to Y-TZP may account for higher strength at the given toughness level which lifts the properties beyond the levels of known strength toughness correlations [19].

5. Conclusions

Alumina toughened zirconia ceramics were manufactured by hot pressing of yttria-neodymia-coated zirconia nanopowder belended with submicron size alumina. The TZP matrix of the ATZ forms a bimodal microstructure with small highly transformable tetragonal grains making up for the majority and large cubic grains of high stabilizer content. Neodymia-yttria co-stabilized alumina zirconia composites may be attractive materials for biomedical implants due to their high strength and toughness and the enhanced resistance to subcritical crack growth under cyclic loading. For best performance an optimization of processing and composition is necessary. Testing the processability of the materials using more performing shaping technologies such as dry pressing coupled with a subsequent pressureless sintering process will be mandatory for a technical implementation of the materials.

References

[1] Begand, S., Oberbach, T., Glien, W.: „ATZ – A New Material with a High Potential in Joint Replacement", Key Eng. Mat., 284-286, (2005), 983-986.

[2] Tsukuma, K., Ueda, K., Shimada ,M.: „Strength and Fracture Toughness of Isostatically Hot-Pressed Composites of Al_2O_3 and Y_2O_3-Partially-Stabilized ZrO_2", J. Am. Ceram. Soc., 68, 1, (1985), C4-5.

[3] Cutler, R.A., Mayhew, R.J., Prettyman, K.M., Virkar, A.V.: „High-Toughness Ce-TZP/Al_2O_3 Ceramics with Improved Hardness and Strength", J. Am. Ceram. Soc., 74, 1, (1991), 179-186.

[4] Kern, F., Gadow, R.: „Properties of Injection Moulded Alumina-Toughened Zirconia", J. Ceram. Sci. Techn., 2, 1, (2011), 47-54.

[5] Kern, F., Gadow, R.: „Alumina toughened zirconia from yttria coated powders", J. Eur. Ceram. Soc., (2012), http://dx.doi.org/10.1016/j.jeurceramsoc.2012.03.014.

[6] Benzaid, R., Chevalier, J., Saâdaoui, M., Fantozzi, G., Nawa, M., Diaz, L.M., Torrecillas, R.: „Fracture toughness, strength and slow crack growth in a ceria stabilized zirconia–alumina nanocomposite for medical applications", 29, Biomaterials, (2008), 3636-41.

[7] Apel, E., Ritzberger, C., Courtois, N., Reveron, H., Chevalier, J., Schweiger, M., Rothbrust, F., Rheinberger, V.M., Höland, W.: „Introduction to a tough, strong and stable Ce-TZP/$MgAl_2O_4$ composite for biomedical applications", J. Eur. Ceram. Soc., (2012), http://dx.doi.org/10.1016/j.jeurceramsoc.2012.02.002.

[8] Vleugels, J., Xu, T., Huang, S., Kan, Y., Wang, P., Li, L., Van der Biest, O.: „Characterization of (Nd,Y)-TZP ceramics prepared by a colloidal suspension coating technique", J. Eur. Ceram. Soc., 27, (2007), 1339-43.

[9] Salehi, S., Van der Biest, O., Vleugels, J.: „Y_2O_3 and Nd_2O_3 co-stabilized ZrO_2-WC composites", J. Mater. Sci., 43, (2008), 5784-89.

[10] Gadow, R., Kern, F.: „Novel Zirconia–Alumina Nanocomposites Combining High Strength and Toughness", Adv. Eng. Mat., 12, 12, (2010), 1220-23.

[11] Kern, F.: „High toughness and strength in yttria-neodymia costabilized zirconia ceramics, Scr. Mat. (2012), http://dx.doi.org/10.1016/j.scriptamat.2012.05.009.

[12] Kern, F.: „2.75Yb-TZP Ceramics with High Strength and Aging Resistance", J. Ceram. Sci. Techn., 2, 3, (2011), 147-54.

[13] Toraya, H., Yoshimura, M., Somiya, S.: „Calibration Curve for Quantitative Analysis of the Monoclinic-Tetragonal ZrO_2 System by X-Ray Diffraction", J. Am. Ceram. Soc., 67, 6, (1984), C119-21.

[14] Braun, L.M., Benninson, S.J., Lawn, B.R.: „Objective Evaluation of Short-Crack Toughness Curves Using Indentation Flaws: Case Study on Alumina-Based Ceramics", J. Am. Ceram. Soc., 75, 11, (1992), 3049-57.

[15] Dransmann, G.W., Steinbrech, R.W., Pajares, A., Guiberteau, F., Dominguez-Rodriguez, F., Heuer, A.H.: „Toughness Determination from Stable Growth of Indentation-Induced Cracks", J. Am. Ceram. Soc., 77, 5, (1994), 1194-1201.

[16] Lube, T., Fett, T.: „A threshold stress intensity factor at the onset of stable crack extension of Knoop indentation cracks", Eng. Fract. Mech., 71, (2004), 2263-2269.

[17] Liu, Z.G., Ouyang, J.H., Zhu, Y., Li, J.: „Effect of alumina addition on the phase evolution and thermal conductivity of ZrO_2–$NdO_{1.5}$ ceramics", J. Alloys Comp., 468, 1-2, (2009), 350-355.

[18] Matsui, K., Yoshida, H., Ikuhara, Y.: „Isothermal Sintering Effects on Phase Separation and Grain Growth in Yttria-Stabilized Tetragonal Zirconia Polycrystal", J. Am. Ceram. Soc., 92, 2, (2009), 467-475.

[19] Swain, M.V., Rose, L.R.F.: „Strength Limitations of Zirconia Toughened Alloys", J. Am. Ceram. Soc., 69, 7, (1986), 511-518.

[20] Chen, M., Hallstedt, B., Gauckler, L.J.: „Thermodynamic modeling of the ZrO_2–$YO_{1.5}$ system", Solid State Ionics, 170, (2004), 255-274.

[21] Wang, C., Zinkevich, M., Aldinger, F.: „Phase diagrams and thermodynamics of rare-earth-doped zirconia ceramics", Pure Appl. Chem., 79, 10, (2007), 1731-53.

♦

Received 29 May 2012; accepted 5 June 2012